CATÓLICA
FACULTY OF BIOTECHNOLOGY
PORTO

QUANTITATIVE SENSOR FOR GLUCOSE MONITORING IN PET'S SALIVA

By:

Maria Francisca Paes Cardoso de Lacerda Aroso

October 2025

CATÓLICA
FACULTY OF BIOTECHNOLOGY
PORTO

QUANTITATIVE SENSOR FOR GLUCOSE MONITORING IN PET'S SALIVA

Thesis presented to *Escola Superior de Biotecnologia of the Universidade Católica Portuguesa* to fulfil the requirements of Master of Science degree in Biomedical Engineering.

By:

Maria Francisca Paes Cardoso de Lacerda Aroso

Place: Escola Superior de Biotecnologia - Universidade Católica Portuguesa

Supervisors: Dr. Raquel Mesquita and Dr. António Rangel

October 2025

“Anyone who tries to improve the lives of animals invariably comes in for criticism from those who believe such efforts are misplaced in a world of suffering humanity.”

— Jane Goodall

Resumo

A diabetes mellitus é uma doença endócrina comum em cães e gatos, cuja monitorização depende tradicionalmente de métodos invasivos através da colheita de sangue, frequentemente associados a desconforto, stress e originando por vezes resultados pouco fiáveis. A saliva tem-se destacado como alternativa não invasiva, permitindo a deteção de biomarcadores como a glucose. Este trabalho teve como objetivo o desenvolvimento e otimização de um dispositivo microfluídico em papel (μPAD) para a determinação quantitativa de glucose na saliva de animais de companhia. O sensor foi concebido a partir de discos de papel tratados com reagentes enzimáticos (glicose oxidase e peroxidase) e o-dianisidina como reagente de cor, permitindo a geração de uma resposta colorimétrica diretamente proporcional à concentração de glucose. Os estudos de otimização focaram-se na escolha do tipo de papel, no volume de amostra e na concentração enzimática, tendo sido alcançados um limite de deteção de 6,7 mg/L e uma gama entre 22,0 e 220 mg/L, abrangendo concentrações fisiológicas e patológicas descritas para cães. O dispositivo apresentou boa reprodutibilidade (RSD = 4%) e custos de produção inferiores a 5€ por unidade. Estudos realizados com amostras de saliva canina confirmaram a capacidade de deteção, embora limitados pelo reduzido número e volume de amostras disponíveis. Assim, o μPAD desenvolvido demonstra-se uma ferramenta promissora para a monitorização não invasiva da glicemia em animais de companhia, contribuindo para um diagnóstico mais acessível, económico e centrado no bem-estar animal.

Palavras-chave: Diabetes mellitus; cães; saliva; biossensores em papel; glucose; diagnóstico não invasivo.

Abstract

Diabetes mellitus is a common endocrine disease in dogs and cats, with diagnosis and monitoring traditionally relying on invasive blood sampling, often associated with stress, discomfort, and inconsistent results. Saliva has emerged as a promising non-invasive alternative for detecting biomarkers such as glucose. This work aimed to develop and optimize a paper-based microfluidic device (μPAD) for quantitative glucose detection in dogs' and cats' saliva. The sensor was designed using layered paper discs loaded with enzymatic reagents (glucose oxidase and peroxidase) and o-dianisidine as a chromogenic substrate, generating a colourimetric response directly proportional to glucose concentration. Optimization studies focused on paper type, sample volume, and enzyme concentration, resulting in a detection limit of 6.7 mg/L and a dynamic range of 22.0 – 220 mg/L, covering both physiological and pathological glucose concentrations in dogs. The device showed good reproducibility (RSD = 4%) and low fabrication costs (< €5 per unit). Tests with canine saliva confirmed the ability to detect glucose, although limited by the reduced number and volume of samples available. Overall, the developed μPAD demonstrates strong potential as a non-invasive tool for monitoring glycemia in pets, supporting more accessible, affordable, and animal-friendly diabetes management.

Keywords: Diabetes mellitus; dogs; saliva; paper-based biosensors; glucose; non-invasive diagnostics.

Acknowledgments

Apesar de este trabalho refletir apenas os últimos sete meses do meu percurso académico, é impossível ignorar o que ele representa no seu todo: cinco anos repletos de vivências e aprendizagens que jamais irei esquecer e que levarei para a vida. Agradecer a todos os envolvidos seria quase impossível, por isso, com muita dificuldade, cinjo-me à seguinte lista.

Em primeiro lugar, não poderia deixar de agradecer à Professora Raquel Mesquita, que me permitiu realizar este trabalho, há tanto desejado por mim, apesar de todas as dificuldades e limitações adjacentes. Sabia, desde o início, que seria um desafio, mas mesmo assim não me disse que não, mantendo sempre a sua postura otimista e assegurando-me de que, no final, eu "iria ter uma história para contar". Agradeço também ao Professor António Rangel, por me permitir integrar temporariamente o seu laboratório, onde cresci profissional e pessoalmente. Não poderia também deixar de referir a enorme presença e importância que ambos os professores tiveram no meu percurso académico, especialmente durante a licenciatura. Foram, sem dúvida, elementos determinantes nestes últimos anos, e por isso lhes estarei eternamente grata.

Gostaria de estender o meu obrigada à Francisca Ferreira, que com muita paciência me acompanhou no laboratório. Para além de me ensinar toda a componente prática, esteve presente em todos os bons e maus momentos, sempre pronta a ajudar e também aturou os meus dramas, fazendo-me sempre ver o copo meio cheio. Um "obrigada" nunca será suficiente.

Agradeço também a todos os restantes elementos do laboratório, que nunca hesitaram em ajudar-me e que proporcionaram sempre um ambiente de trabalho descontraído e agradável.

Não poderia deixar de agradecer aos meus pais, por estarem ao meu lado em todas as decisões e por terem sido, desde sempre, os meus maiores pilares. Obrigada pelo apoio incondicional, pela paciência nos momentos de dúvida e pela força que me acompanhou em cada etapa. Sem eles, jamais teria conseguido.

Aos meus avós, que acompanharam todo este percurso e acreditaram sempre no meu sucesso.

Obrigada a todos os meus amigos, em especial ao Gabriel, à Leonor e às Ritas, cuja amizade me acompanhou desde o início até ao fim desta jornada. Obrigada por estarem sempre presentes, por acreditarem em mim e no potencial deste trabalho, por cada palavra de incentivo e por me lembrarem de celebrar as pequenas vitórias.

Não poderia deixar de agradecer a todos os colegas que se cruzaram no meu caminho, que me apoiaram, partilharam desafios e conquistas, e tornaram esta experiência académica mais leve e bonita.

Ao Gaudi, motivação deste trabalho, que não chegou a tempo de ser a minha cobaia, mas que, sem dúvida, teria sido um entusiasta de um mundo onde a medicina veterinária fosse menos invasiva. O seu amor e lealdade foram um alicerce silencioso de grande parte deste percurso, e a sua memória permanecerá sempre comigo.

Por fim, agradeço à Escola Superior de Biotecnologia, que foi a minha casa nos últimos anos e que me proporcionou excelentes oportunidades. Guardarei para sempre todos os momentos vividos.

Contents

1. Introduction

1.1. Medical and Scientific Framework

Glucose is a simple carbohydrate and the principal energy source for cellular metabolism. It is absorbed in the small intestine and carried into the bloodstream, where it is metabolized through glycolysis to provide energy to various tissues. Hormonal regulation, mostly including insulin and glucagon, keeps blood glucose levels within a specific physiological range. Disruption of this balance, as observed in diabetes, results in chronic hyperglycemia and other systemic consequences [1]. Because chronic high blood sugar levels negatively impact several organ systems, routine glucose monitoring is crucial for precise diagnosis, effective therapy, and long-term management of illnesses [1].

Diabetes mellitus is a prevalent endocrine illness in dogs and cats, and its incidence has risen in recent years. It is estimated that approximately 0.2% to 0.5% of dogs and around 0.5% of cats are affected by the disease [2]. Diabetes in dogs usually resembles human type 1 diabetes because of the immune system's destruction of the pancreatic β-cells and the resulting insulin shortage. Cats exhibit insulin resistance and β-cell dysfunction, similar to human type 2 diabetes, which is commonly linked to obesity, advanced age, and sedentary lifestyles (Figure 1) [3,4].

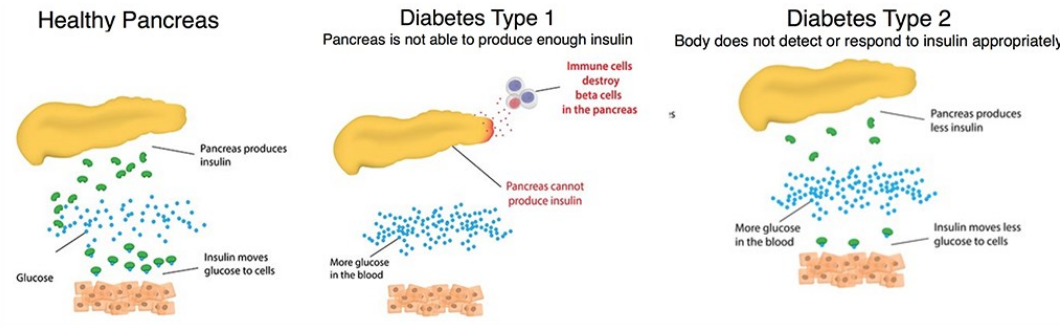

Figure 1: Visual comparison of glucose regulation in healthy animals and animals with Type 1 or Type 2 diabetes [5].

Long-term care and an accurate diagnosis are essential for minimizing issues and improving quality of life. However, regular blood collection is a major component of conventional diagnostic techniques, which can be invasive, stressful, and provide inaccurate results, especially in cats, where stress-induced hyperglycemia can mimic diabetes profiles [3,6].

Table 1 : Blood Glucose Reference Ranges in Dogs and Cats [3]

Species	Normal Blood Glucose (mg/dL)	Diabetic Glucose (mg/dL)
Dog	75-120	>180-220
Cat	70-130	>180-220*

*Note: Feline values may be influenced by stress hyperglycemia

The 2022 American Animal Hospital Association (AAHA) Guidelines state that a dog's normal fasting blood glucose range is 75–120 mg/dL, whereas a cat's normal range is 70–130 mg/dL (Table 1). These thresholds are clinically important for diabetes monitoring since hyperglycemia above ~200 mg/dL in dogs or 250–300 mg/dL in cats causes glucosuria, the presence of glucose in urine [3]. This outcome has important clinical implications, as urinary glucose reflects blood glucose concentrations exceeding the renal threshold, which may cause osmotic diuresis, dehydration, electrolyte disturbances, and predispose diabetic dogs and cats to urinary tract infections [7].

The 2022 AAHA Diabetes Management Guidelines acknowledge the limitations of currently available instruments and emphasize the importance of consistent and frequent glucose monitoring [3]. While continuous glucose monitoring (CGM) systems, such as the FreeStyle Libre, an interstitial glucose sensor applied to the skin that provides nearly continuous readings for up to 14 days, provide a minimally invasive and data-rich way to track glycemic trends, sensor detachment, lower accuracy during hypoglycemia, and improper use continue to limit its applications in veterinary medicine. These systems measure glucose in the fluid surrounding body tissues, which can lag slightly behind blood glucose levels during rapid changes. Furthermore, gadget malfunctions and brief wear times are frequent occurrences, which call for clinical supervision and possible confirmation with conventional glucose testing [3].

Saliva has been emerging as a promising biological matrix for obtaining non-invasive and stress-free samples in dogs. Although concentrations are lower than in serum and there is a noticeable delay in response, recent studies have demonstrated that insulin and glucose may be accurately detected in canine saliva after glucose delivery [8]. Therefore, the creation of a quantitative, paper-based diagnostic tool for salivary glucose detection presents a viable, quick, economical, and animal-friendly alternative to invasive blood

sampling in pet diabetes monitoring, potentially reducing the need for regular medical compliance on the part of owners (Figure 2).

Figure 2: Comparison of glucose monitoring methods in animals, including traditional blood sampling, continuous glucose monitoring (CGM), and emerging saliva-based testing.

1.2. Non-Invasive Diagnostic Alternatives

Blood draws and urine collection are frequently used in veterinary diagnostic procedures, which can be both physically challenging and stressful for animals. These techniques typically require specialized staff and physical restraint, which can elicit physiological reactions such as cortisol spikes or altered glucose levels, potentially compromising the accuracy of the diagnosis. Saliva, on the other hand, has shown great promise as a biological fluid for diagnostic applications due to its non-invasiveness, convenience of sample, and reduced stress impact.

For instance, after being exposed to stress, dogs' salivary cortisol concentrations and plasma cortisol levels are strongly correlated [9]. Additionally, during simulated field operations, both rescue dogs and their handlers experienced a rise in salivary cortisol levels, demonstrating the sensitivity of saliva as a biomarker for acute stress [10]. These findings emphasize that saliva is not only a stress-free matrix for hormone monitoring but also a biologically informative one.

Before the veterinary use, saliva was also being investigated more and more in human healthcare for the detection of systemic diseases such as infections, metabolic abnormalities, and hormone imbalances. Salivary diagnostics' sensitivity and reliability have been greatly increased by recent technical developments, especially in the fields of

microfluidics and biosensing, which have encouraged their wider clinical application [11]. Nevertheless, some restrictions continue to prevent their general use. These include lower biomarker concentrations compared to blood; possible sample contamination from food, bacteria, or oral health issues; high viscosity that can make handling more challenging; and variations in salivary composition resulting from circadian rhythms, hydration levels, and individual physiology. Furthermore, extensive clinical validation is still needed for several suggested salivary biomarkers [11]. Although saliva has a lot of potential for non-invasive diagnostics in veterinary care, these drawbacks apply to animals just as much, if not more. To overcome them, more pet-specific validation studies, standardized procedures, and species-specific research are needed.

In dogs, no single saliva-collecting technique may be regarded as ideal, despite some research suggesting that passive drooling and synthetic swabs are less upsetting and frequently successful. The technique chosen needs to be customized to the goals of the study, the target analytes, and the traits of the canine participants [12]. In the present work, saliva samples were collected using different approaches depending on the circumstances and animal behavior, although the specific collection methods were not consistently documented.

1.3. Paper-Based Sensors and Microfluidic Devices

Paper-based diagnostic devices date back to the mid-twentieth century, with the introduction of the first colourimetric test strips in 1956. These early techniques allowed for the visual determination of analyte concentrations through simple enzyme-mediated reactions on paper. Microfluidic paper-based analytical devices (μPADs) have emerged from the evolution of paper-based formats over time. μPADs are a low-cost, field-deployable platform that combines passive fluid transport, small microchannel design, and multiple detection modalities [13]. Colorimetric detection using μPADs can be qualitative, offering a simple yes/no response; semi-quantitative, based on visual assessment of color gradients; or fully quantitative, through image analysis software [14]. Their capillary-driven flow, structural flexibility, and compatibility have expanded their use beyond traditional diagnostics to include environmental monitoring, food safety, and

agricultural applications, signaling a significant shift from single-use test strips to multifunctional analytical systems.

The fundamental principle of paper microfluidics is capillary action, which allows liquids to flow through porous materials on their own without the need for additional pumps or power sources. A network of microchannels formed by the cellulose fibers in paper directs fluid flow in a regulated and predictable way. Certain microfluidic paths can be created to direct fluids into detection zones or reaction sites by patterning hydrophobic barriers using methods like photolithography, inkjet printing, or wax printing (Figure 3) [13,15].

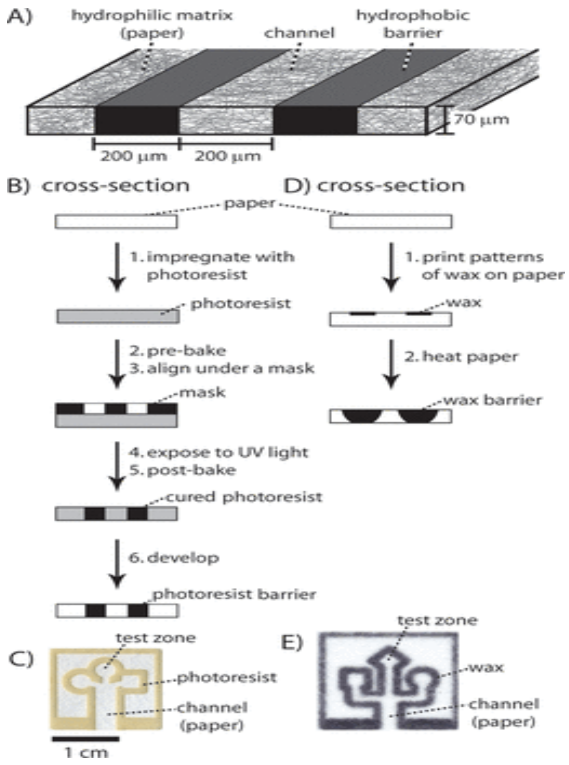

Figure 3: Comparison of photolithographic (left) and wax printing (right) µPAD fabrication. (A) Hydrophilic channels and hydrophobic barriers. (B–C) Photolithography process and design. (D–E) Wax printing process and layout [15].

µPADs are a promising solution for quantitative glucose monitoring in low-resource or field settings. These systems typically use enzymatic reactions involving glucose oxidase (GOx) to turn glucose into hydrogen peroxide, which is then detected using colourimetry (Figure 4) or electrochemistry [13,17]. Colourimetric µPADs, formed by reactions with potassium iodide, o-dianisidine, or 3,3',5,5'-tetramethylbenzidine (TMB), can be used to correlate glucose concentration with printed colour scales or mobile phone picture analysis [15,18,19].

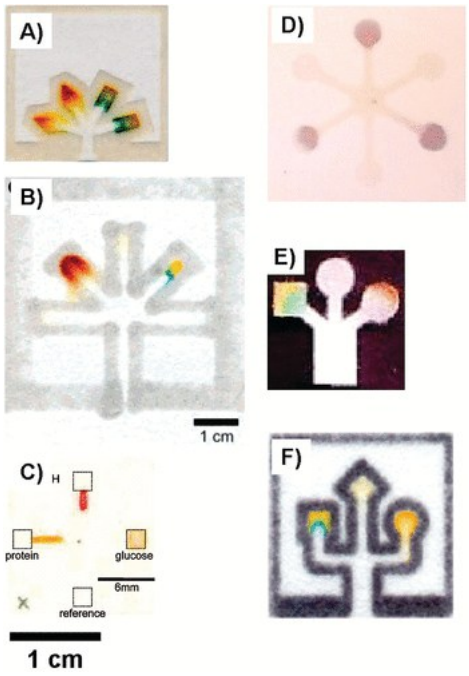

Figure 4: Examples of colourimetric µPADs used for biochemical analysis.

Although not totally quantitative, this approach allows for the accurate classification of glucose levels into relevant ranges, which is especially useful for on-site monitoring in healthcare environments [13,20]. Electrochemical µPADs, featuring screen-printed electrodes on paper, offer enhanced sensitivity and dynamic range, enabling precise semi-quantitative analysis [16,21]. Particularly for field use and animal health diagnostics, µPADs are a strong substitute for conventional glucose meters due to their capacity to store reagents in dry form in advance, function without the need for additional pumps, and be read visually or electronically [13,17,20]. Similar µPAD-based techniques have also been used to detect urease, urea, and ammonium in human saliva, demonstrating the versatility of these platforms for various biological fluids and enzymatic targets [22,23].

µPADs are developed by selectively creating hydrophilic channels and hydrophobic barriers using techniques such as photolithography, inkjet printing, plasma etching, and wax printing [13,15,16]. While inkjet and photolithographic techniques offer more control at the cost of complexity, wax printing remains widely used due to its affordability and ease of access [15,24].

µPADs are classified as two-dimensional (2D) or three-dimensional (3D) based on their structural design and fluidic flow pathways (Figure 5). 2D µPADs consist of a single planar layer with hydrophilic channels patterned on paper, enabling lateral capillary flow and making them suitable for simple assays. In contrast, 3D µPADs are created by folding

a single sheet (origami approach) or stacking multiple layers, allowing fluid to flow vertically between layers (Figure 6). This architecture supports more complex analytical functions, including multistep reactions, improved reagent storage and delivery, spatial isolation of assay zones, and sequential fluid manipulation, all of which improve the device's effectiveness when performing multiple tests simultaneously or when precise timing and sequencing of reactions are required [24].

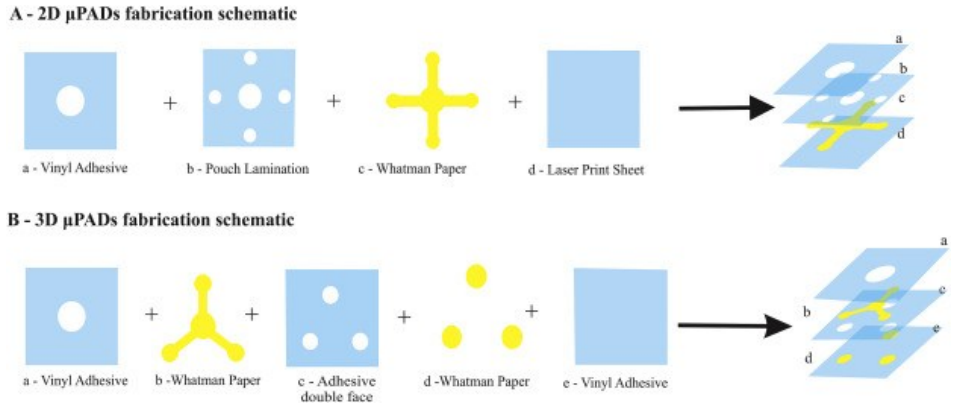

Figure 5: Schematic comparison of 2D and 3D µPAD fabrication techniques [26].

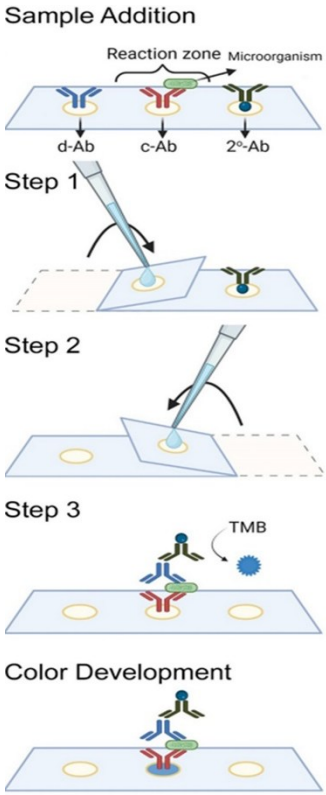

Figure 6: Origami µPAD for sequential sample delivery and colorimetric detection [27].

Both geometric patterns and chemical interventions are used to control flow. Geometry-based control techniques adjust fluid velocity and time, including changing the length or breadth of the channel, adding shunts or hollow portions, and using 3D or origami designs [16,28]. Chemical-based techniques include the use of viscous sugar coatings, flow diodes or valves that enable multistep tests independently, and incorporating dissolvable barriers such as trehalose or sucrose [20,17].

Furthermore, dynamic control over flow start and sequencing is possible through methods such as plasmon-inscribed flow diodes and pressure modulation, which involves manually compressing paper channels [28]. These developments, when paired with passive capillary wicking, allow for multiplex detection, multistep reagent delivery, and complex assay formats in portable paper-based devices, all of which successfully meet the ASSURED (Affordable; Sensitive; Specific; User-friendly; Robust and Rapid; Equipment-free and Deliverable to those who need them) guidelines by WHO (World Health Organization), for field diagnostics and glucose monitoring applications [13,15,20].

Although promising, microfluidic paper-based analytical devices still have technical and practical limitations. Low sensitivity, poor repeatability, and limited operational shelf life are some of the most significant limitations, particularly when used with complex biological matrices like animal fluids or subjected to a variety of environmental conditions [29,30]. Furthermore, widespread acceptance and regulatory approval have been inhibited by the absence of consistency in manufacturing techniques, reagent deposition, and result interpretation [29,31].

Current research is investigating the integration of nanomaterials (such as graphene oxide and gold nanoparticles) to improve assay stability and detection sensitivity to get around these restrictions [31]. The use of synthetic recognition elements and enzyme-free detection systems is another possibility that can enhance the durability and robustness of μPADs in challenging field settings [31]. In the meantime, digital integration is becoming more popular as a means of improving result dependability and facilitating real-time data collection, such as smartphone-based photography and AI-assisted quantification (Figure 7) [32]. To address sustainability problems in large-scale production, the sector is also shifting toward greener materials and fabrication procedures [31].

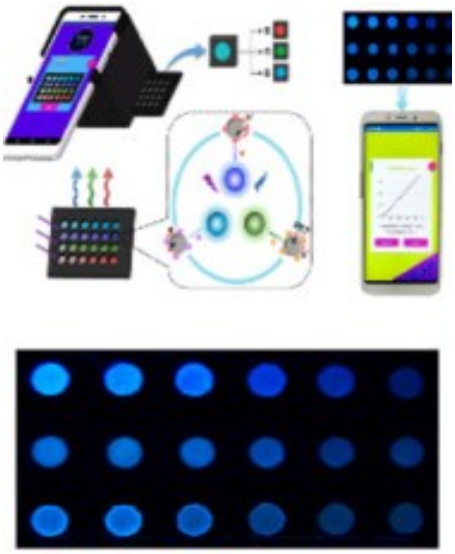

Figure 7: Example of smartphone-based detection integration in a paper-based analytical device [32].

In the future, analytical performance, affordability, ease of use, and environmental resilience will all need to be addressed in µPAD systems. Achieving this will likely require advances in multiplexed detection, programmable fluid control, and modular µPAD designs, such as origami-based or stackable formats. Transforming µPADs from lab-scale prototypes into fully functional diagnostic tools for human and veterinary applications would require addressing these issues through cross-disciplinary collaboration and regulatory standardization [29,33].

1.4. Objectives

The primary objective of this work was to develop a paper-based microfluidic device capable of measuring glucose levels in a pet's saliva. The device was designed for both clinical and at-home use, aiming to provide a low-cost, non-invasive alternative to conventional blood glucose testing. By focusing on saliva, this work supports earlier diagnosis and improved disease management through promoting stress-free diabetes monitoring in dogs and cats. In this way, it contributes to improved welfare and long-term care for diabetic pets by meeting the growing need for animal-friendly diagnostics.

To achieve this, a µPAD was developed based on a previously described method by Ferreira et al. (2024) [34]. The detection relied on a two-step enzymatic reaction using a mixture of glucose oxidase and peroxidase, with o-dianisidine as the chromogenic

reagent. Glucose is oxidized by glucose oxidase, producing gluconic acid and hydrogen peroxide (H_2O_2). In the presence of peroxidase, H_2O_2 oxidizes o-dianisidine, resulting in a brown-coloured product. Upon acidification with sulfuric acid (H_2SO_4), the oxidized o-dianisidine shifts to a pink form, allowing for enhanced colourimetric quantification (Figure 8) [35].

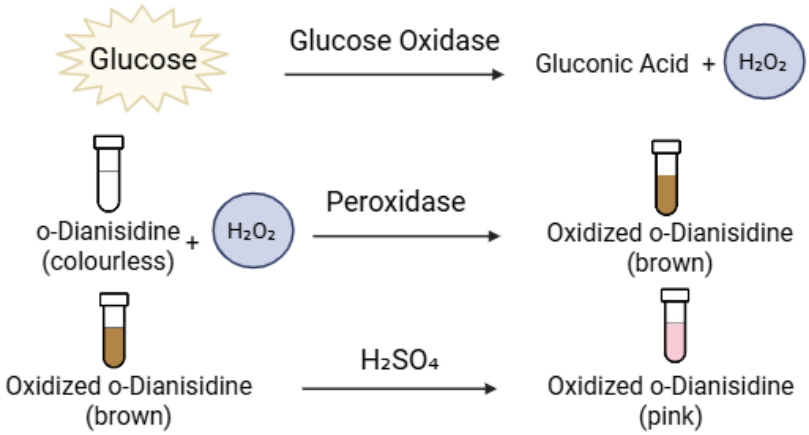

Figure 8: Schematic representation of the enzymatic colourimetric reaction used for glucose detection.

Due to the limited information available on glucose concentrations in animal saliva, the glucose range used for the µPAD was guided by data from Muñoz-Prieto et al. (2019) [8], which reported salivary glucose levels between approximately 2.5 mg/dL in non-diabetic and 25.5 mg/dL in diabetic dogs. The selected calibration standards (2.20, 4.40, 8.80, 13.2, and 22.0 mg/dL) not only encompass but also slightly exceed this physiological range, ensuring appropriate sensitivity and accurate quantification across the expected concentration levels.

2. Materials and Methods

2.1. Reagents and Solutions

A 2.20 g/L glucose stock solution was freshly prepared each month by dissolving 22 mg of D(+)-glucose anidro (Merck) in 10 mL of distilled water. This stock was divided into 10 aliquots, each containing 1 mL of the solution, and then frozen. Each week, 5 standards ranging from 22.0 to 220 mg/L were prepared from 1 mL aliquots.

An acetate buffer (0.05 M, pH 5.0) was made by dissolving 446 mg of sodium acetate (CH_3COONa, Merck) in 100 mL of water, followed by pH adjustment.

A 0.1 M phosphate buffer was prepared by dissolving 114 mg of di-Potassium hydrogen phosphate trihydrate ($K_2HPO_4 \cdot 3H_2O$, Merck) in 5 mL of water, with pH adjusted to 6.0.

All buffers were kept refrigerated when not in use.

The glucose oxidase (GOx, from *Aspergillus niger*, Type VII, Sigma-Aldrich) stock solution was made by dissolving 3 mg of enzyme in 1 mL of 50 mM acetate buffer, resulting in a concentration of 750 U/mL. This solution was stored frozen, according to the manufacturer's instructions, and diluted daily to 158 U/mL.

The peroxidase (Pox, from horseradish, Type I, Sigma-Aldrich) stock solution at 800 U/mL was prepared by dissolving 9 mg of enzyme powder in 1 mL of the 0.1 M phosphate buffer. A daily dilution was performed using 50 mM phosphate buffer to achieve a final activity of 165 U/mL.

Just before device assembly, the enzymatic mixture was freshly prepared by mixing GOx (158 U/mL), Pox (165 U/mL), and 100 mM phosphate buffer in equal volumes (1:1:1). The final GOx and Pox concentration was 52.6 U/mL and 55.0 U/mL, respectively

A 4 mM stock solution of o-dianisidine was prepared monthly by dissolving 10 mg of the compound (Sigma-Aldrich) in 10 mL of 96% ethanol. This was diluted every two weeks in water to yield a 1 mM solution containing 24% ethanol.

Synthetic saliva was prepared according to Batista et. al (2016) [36] with the following composition: [KCl] = 2.24 g/L; [KH_2PO_4] = 0.54 g/L; [$CaCl_2 \cdot 2H_2O$] = 77.7 mg/L; [$MgCl_2$] = 19.4 mg/L; [HEPES] = 4.77 g/L; [Bovine Serum Albumin (BSA), instead of mucin] = 2.70 g/L.

All solutions used in this study were prepared using analytical-grade reagents and Milli-Q ultrapure water (resistivity < 18 MΩ·cm; Millipore, Burlington, MA, USA).

2.2. Design of the developed µPAD

Each µPAD was configured using a 75 × 110 mm plastic laminating pouch (Q-Connect) serving as the hydrophobic layer. The pouch was perforated with twenty-four holes (3 mm in diameter) to enable sample application (laser cutting machine, FDA, Model 3040). Directly beneath each hole, the filter paper discs were placed to form the hydrophilic region. These discs were arranged in a 6-column by 4-row grid layout, corresponding to 24 reading units.

Three layers of filter paper were used and assembled (fig 9A) to form each detection unit (fig 9B). The first layer (bottom), made of Whatman Grade 50 paper with a diameter of 1,27cm, was loaded with 18 µL of o-dianisidine and dried in the oven (Memmert U30) at 55 °C for 10 minutes. The second layer (middle), consisting of Whatman Grade 42 paper (9,5 mm in diameter), was treated with 15 µL of the glucose oxidase and peroxidase (GOx + Pox) enzyme mixture and also dried at 55 °C for 10 minutes. The third layer (top), made of Whatman Grade 1 paper (also 9,5 mm diameter), remained empty and served as a protective cover. After drying the discs with reagents, the layers were aligned and assembled into the reading units, which were then placed into the laminating pouches. The pouches were then passed through a laminator (REXEL Style A4), resulting in a µPAD with a hydrophobic region provided by the plastic film and a hydrophilic reaction zone formed by the stacked paper discs. A volume of 25 µL from each of the five glucose standard solutions (22.0, 44.0, 88.0, 132, and 220 mg/L), along with a blank sample (water), was applied to the corresponding holes in the laminated pouches (Fig 9C). To prevent contact with the targeted biological fluid, the holes were sealed with adhesive tape after the samples had been fully absorbed and dried. The underside of the µPAD was then scanned after 30 minutes, the time it took the standards/samples to dry completely.

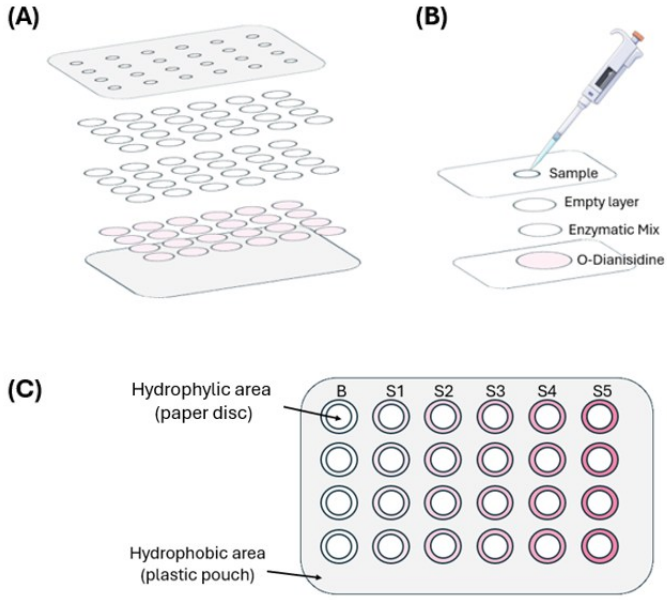

Figure 9: Glucose µPad assembly; (A) Schematic representation of the stacking; (B) Representation of a single reading zone, with a sample volume of 25 µL showing the three-part structure of each reaction zone: o-dianisidine layer (bottom), enzymatic mix layer (middle), and a protective empty layer (top); (C) Top view of the final laminated µPAD containing 24 detection zones, including one blank (B) and five different standards (S1–S5).

2.3. Image and Data Analysis

The enzymatic and colourimetric reaction occurring in the µPAD, involving glucose, the enzyme mixture (GOx + Pox), and o-dianisidine, results in the formation of a pink-coloured product. The intensity of the pink colour is directly proportional to the glucose concentration in the sample; that is, the stronger the colouration, the higher the glucose level. To quantify this color development, the underside of the µPAD was scanned using a standard scanner (Epson Stylus SX100). The scanned images were processed using ImageJ software. Through the "RGB stack" function, each image was split into its red, green, and blue channels, as the acronym suggests. The pink colouration corresponds to specific patterns of light absorption and reflection. Since the complementary colour of pink is green (Figure 10), an increase in pink intensity corresponds to greater absorption in the green spectrum. Therefore, the green channel was selected for image analysis, enabling quantification based on colour intensity.

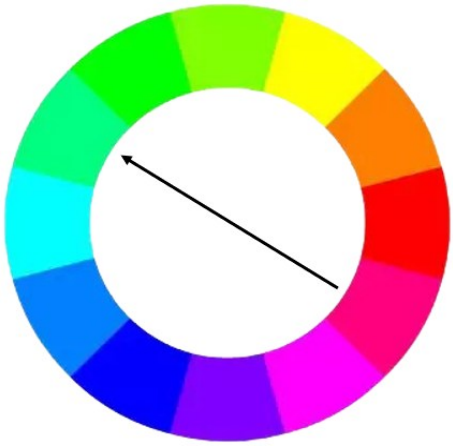

Figure 10: RGB-based colour wheel showing the complementary relationship between magenta/pink and green.

To quantify the colour intensity of each disc, the circular selection tool in ImageJ was used, with a fixed height and width of 46 pixels, ensuring consistent alignment with each disc. The intensity of all 24 discs was measured using the "M" command, generating a results table that included the measured area, as well as the maximum, minimum, and mean intensity values. The mean intensity values for each disc were then converted into absorbance values using the formula: $A = \log(I_0/I)$, where A is the absorbance, I is the mean intensity of the sample (based on four replicates per standard), and I_0 is the mean intensity of the blank (also four replicates). This approach allowed the construction of a calibration curve correlating glucose concentration with the absorbance values obtained.

Figure 11: Workflow of µPAD colourimetric analysis and calibration curve generation.

2.4. Saliva sample collection and preparation

A total of four saliva samples were used, all obtained from dogs. Each sample had a limited volume, which influenced the determination analysis. The method of collection was not standardized, and each pet owner did as they managed. Samples were transported and subsequently stored frozen before analysis.

2.5. Comparative procedures

Additional comparative test procedures were performed with diluted and spiked saliva samples, prepared as described in Table 2. These assays were conducted using the Megazyme D-Glucose HK Assay Kit [37] according to the manufacturer's protocol.

Table 2: Preparation of the saliva samples.

Sample ID	Sample Amount	Sample Dilution	Volumes (µL)	Total Volume (µL)
A1	50 µL of dog saliva (sample A)	250 µL of glucose standard in synthetic saliva (22 mg/L)	50 + 250	300
A2	150 µL of A1	50 µL of glucose standard in water (220 mg/L)	150 + 50	200
B1	100 µL of dog saliva (sample B)	200 µL of glucose standard in synthetic saliva (22 mg/L)	100 + 200	300
B2	150 µL of B1	50 µL of glucose standard in water (220 mg/L)	150 + 50	200

3. Results and Discussion

3.1. Preliminary studies

Before the optimization of the μPAD to be developed, some preliminary spectrophotometric tests were carried out to evaluate the best conditions for the enzymatic reaction, namely the buffer used. The enzyme mixture used for glucose detection, composed of glucose oxidase and peroxidase, can be prepared in either acetate or phosphate buffer, according to the manufacturer's instructions. However, to simplify by using just one buffer, a comparative assessment was conducted to determine which buffer provided better performance in terms of sensitivity.

Standard glucose solutions were prepared in both buffers and tested under identical conditions (1 mL of buffer + 1 mL of glucose standard + 1 mL of o-dianisidine + 0.1 mL of enzyme mix). Colour intensity was measured at 450 nm using a spectrophotometer (Hitachi 100-40). The calibration slopes obtained using the two buffers showed that the phosphate buffer produced a higher slope value (1.80 g/L) compared to acetate (1.12 g/L), indicating greater analytical sensitivity for glucose detection (Figure 12). Based on these findings, the phosphate buffer was selected for all subsequent experiments.

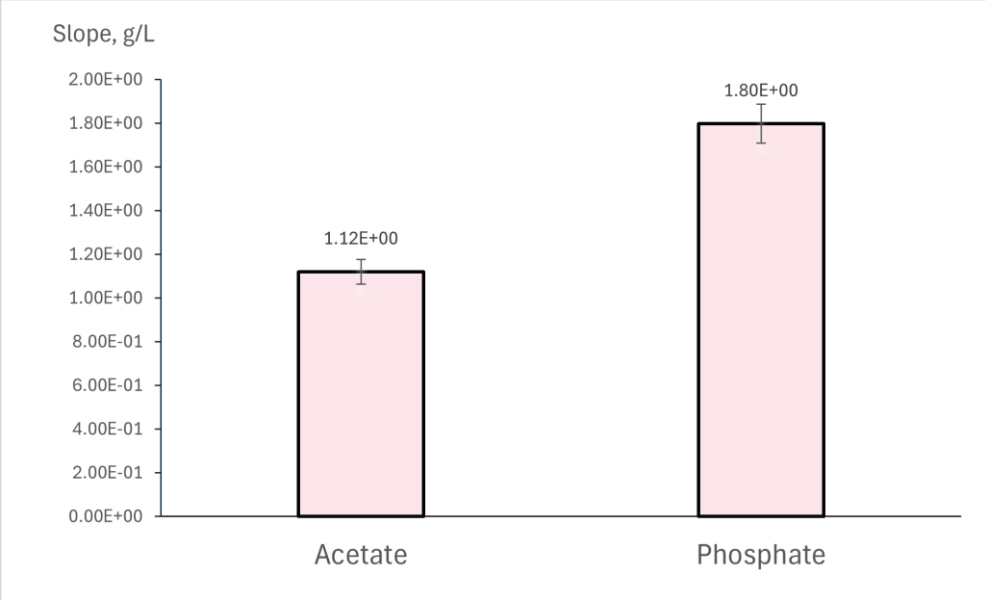

Figure 12: Sensitivities of the calibration curves prepared using the two different buffers in a batchwise procedure.

3.2. Glucose Determination and Optimization Studies

3.2.1.First design of the μPAD

Following the buffer selection experiments, the development and optimization of the μPAD were the next steps. As previously mentioned, the initial design was adapted from a μPAD previously developed by Ferreira et al. (2024), [34] in which a laminated pouch served as the hydrophobic structure, and 24 filter paper discs were used as hydrophilic zones where the enzymatic reaction takes place.

In the initial version, each reading unit was composed of two layers: one containing the chromogenic reagent and the other containing the enzyme mixture. However, it was observed that the laminating process, due to the high operating temperatures, damaged the enzymatic mix layer as a consequence of enzymes being highly sensitive to heat. The resulting thermal degradation compromised their activity, and no visible colour change was observed.

To address this issue, an additional empty paper layer was introduced on top of the enzymatic layer to protect it from direct heat exposure during lamination. This adjustment not only preserved enzymatic activity but also allowed for a larger sample volume to be applied to each disc.

The incorporation of this third layer markedly improved sensitivity compared to the two-layer configuration (Double), as shown in Figure 13, confirming its protective role and the benefit of enabling the application of a 25 μL sample volume.

3.2.2. Filter paper and sample volume optimization

Following optimization studies focused on selecting the most appropriate type of filter paper for this protective layer, as well as determining the optimal sample volume. These resulted in a final μPAD configuration consisting of three paper layers per disc and a sample volume of 25 μL, with complete drying achieved in approximately 30 minutes.

Different pore sizes of qualitative grade filter paper from Whatman (W1, W3, W4) were evaluated as candidates for this protective layer, selected based on their structural and physicochemical properties (Appendix A). The results demonstrated that Whatman Grade 1 yielded the highest sensitivity (1.31×10^{-4} L/mg), followed by Grade 4 (1.26 ×

10^{-4} L/mg). By contrast, Grade 3 showed highly variable responses depending on the applied sample volume: 3.74×10^{-5} L/mg at 25 µL, 1.17×10^{-4} L/mg at 30 µL, and 4.41×10^{-5} L/mg at 35 µL. Higher volumes were tested only on Grade 3 due to its thickness.

The best performance of Grade 1 can be attributed to its relatively low thickness (180 µm), moderate particle retention (11 µm), and high porosity, which favour efficient sample permeation and reagent interaction while still providing adequate protection against heat. Grade 4 performed comparably to Grade 1, though its slightly higher thickness (205 µm) and lower porosity likely restricted diffusion to some extent. Conversely, Grade 3, with its greater thickness (390 µm) and lower air flow rate (26 s/100 mL/in²), may have limited fluid penetration and slowed reaction kinetics, thereby reducing sensitivity despite the increased sample volume.

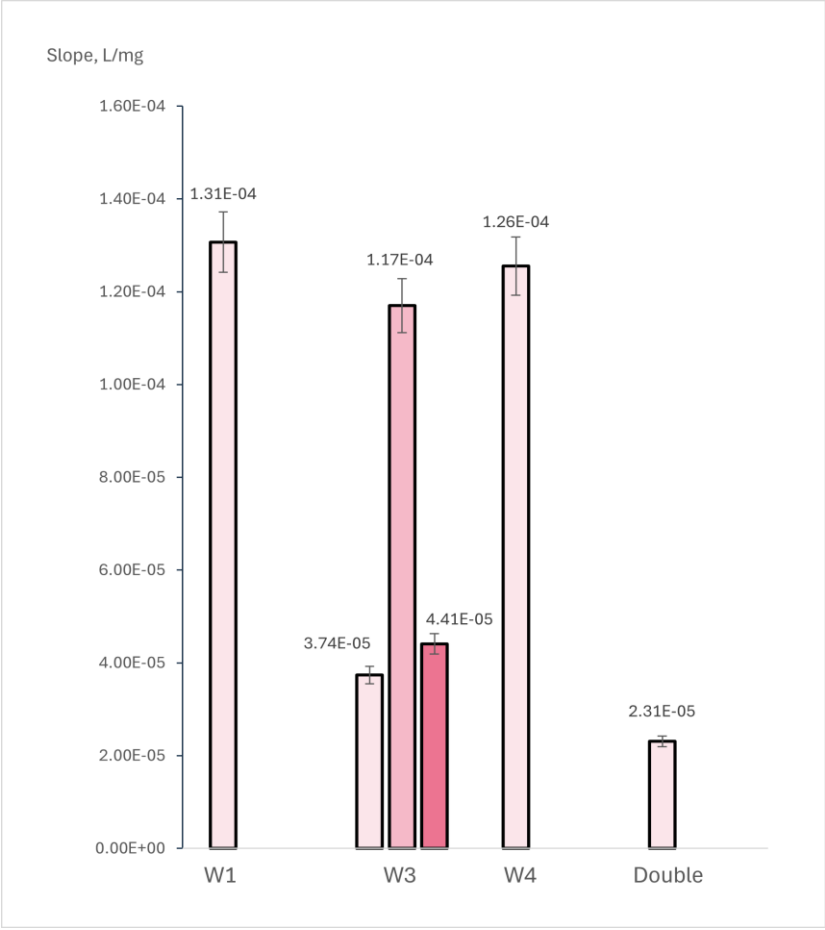

Figure 13:Sensitivity values obtained with different protective filter papers (W1, W3, and W4) compared to the two-layer configuration (Double). The sample volume was 25 µL, except for W3, where additional volumes of 30 µL (medium pink) and 35 µL (dark pink) were also evaluated.

3.2.3.Enzyme Mix volume optimization

In the preliminary studies, the enzymatic mix was used in a diluted form ([Gox]= 26.3 U/mL; [Pox]=27.5 U/mL). To see if a higher concentration of enzyme would increase the sensitivity, the original, non-diluted preparation ([Gox] = 52.6 U/mL; [Pox]= 55.0 U/mL) was applied, and a significant change was observed (Figure 14). The slope value increased from 2.82E-04 L/mg with the diluted mix to 3.84E-04 L/mg with the original one, corresponding to an improvement of approximately 36%. Such results suggest that enzyme dosage plays a crucial role, as insufficient concentrations may limit the oxidative cross-linking reactions promoted by the GOx+Pox mix, thereby reducing their technological impact.

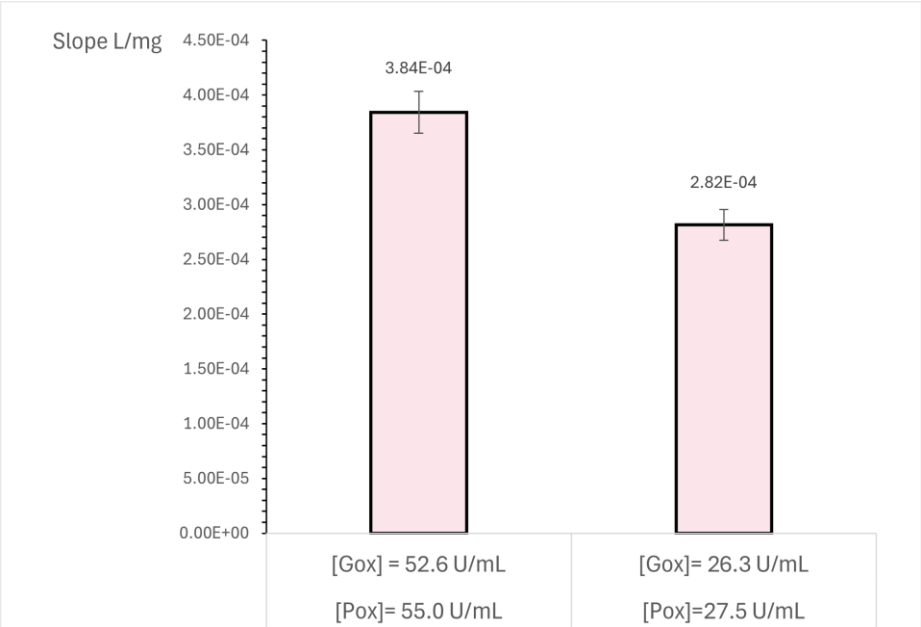

Figure 14: Sensitivity comparison between the undiluted and diluted enzyme mix.

3.3. Interference Assessments

To evaluate the possible matrix interferences, two sets of glucose standards were prepared, one in synthetic saliva and one in water. As shown in Figure 15, the sensitivity values were 3.10×10^{-4} L/mg (water) and 2.98×10^{-4} L/mg (synthetic saliva), corresponding to a difference of ~4%. Since this variation was not significant, subsequent calibrations were performed in water, which simplified the procedure and reduced reagent consumption.

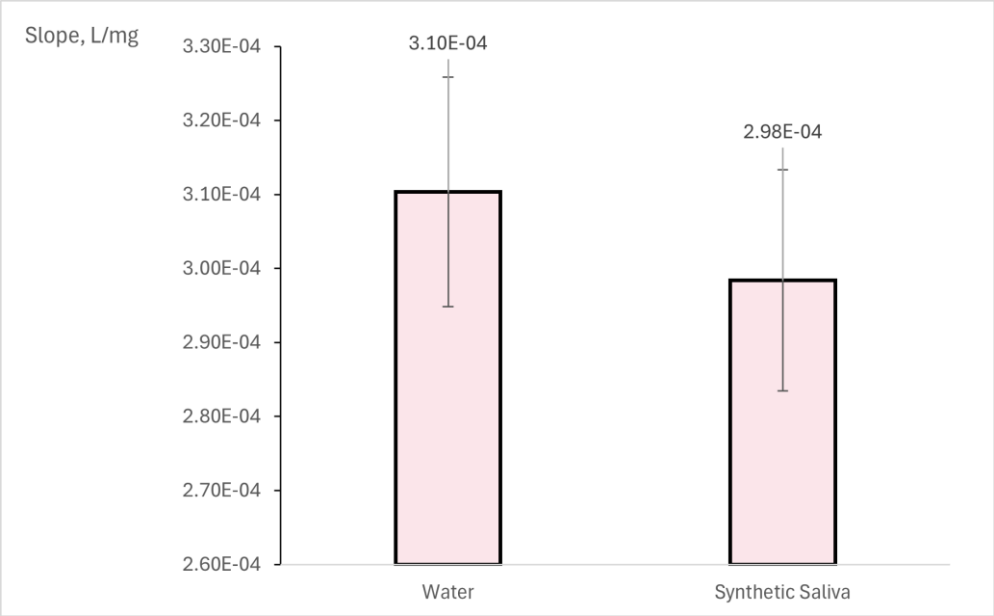

Figure 15: Sensitivity values obtained with glucose standards prepared in water and synthetic saliva.

3.4. Stability Studies

To assess the durability of the developed µPADs, stability tests were carried out considering two aspects: the stability of the devices during storage before sample application, and the stability of the coloured product generated.

3.4.1. Stability of µPAD

The stability of the developed µPADs was systematically evaluated under different storage times and conditions, and the results are presented in Figure 16. The pink shaded region represents the ±5% deviation relative to freshly prepared devices, which was considered the acceptance interval for stability.

For the short-term period, devices stored either under air or vacuum for up to 3 days exhibited sensitivity values that remained within this acceptance interval, demonstrating that the µPADs preserved their analytical performance during the initial days after fabrication. This is particularly relevant for practical applications, as it indicates that the devices can be prepared in advance and used shortly thereafter without significant loss of activity.

However, after 7 days of storage, a clear decline in sensitivity was observed, with values falling well below the ±5% range. This effect became even more pronounced after 15 days, suggesting a progressive degradation of the enzymatic system or possible alterations in the microfluidic structure over time. Factors such as gradual enzyme inactivation, diffusion of reagents within the paper matrix, or changes in the hydrophilic properties of the substrate may explain this loss of activity.

Notably, when storage time was extended to 30 days, devices maintained under vacuum and at low temperature showed sensitivity values that again aligned with the acceptance criteria, close to those of freshly prepared µPADs. In this way, it is possible to conclude that vacuum and temperature conditions may contribute to reducing degradative processes, for example, by limiting oxidation or moisture uptake, thus contributing to longer shelf-life.

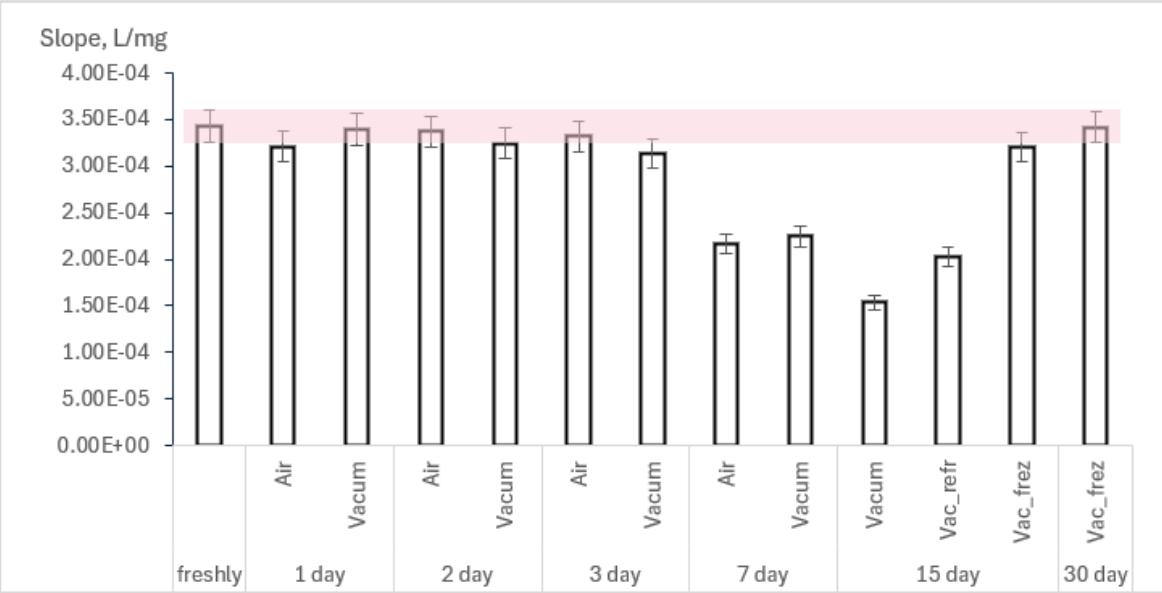

Figure 16: Stability of µPADs over different storage times and conditions. The shaded area represents the ±5% deviation relative to freshly prepared devices.

3.4.2. Stability of the coloured product

The stability of the coloured product formed after sample application was monitored over 24 hours (Figure 17). At 30 minutes, the µPADs already exhibited a measurable calibration slope (3.40×10^{-4} L/mg), representing the minimum analytical sensitivity required for reliable quantification. The slope progressively increased, reaching its

maximum at around 2 hours (5.25×10^{-4} L/mg). Beyond this point, values remained stable, with no significant variation up to 24 hours (5.61×10^{-4} L/mg).

These results indicate that the chromogenic reaction continues to develop during the first 2 hours, after which the analytical response stabilizes without evidence of degradation. This suggests that µPADs can provide consistent readings from 30 minutes onwards, with the optimal sensitivity achieved after approximately 2 hours. For practical point-of-care applications, however, the 30-minute reading represents a suitable compromise between analytical performance and usability.

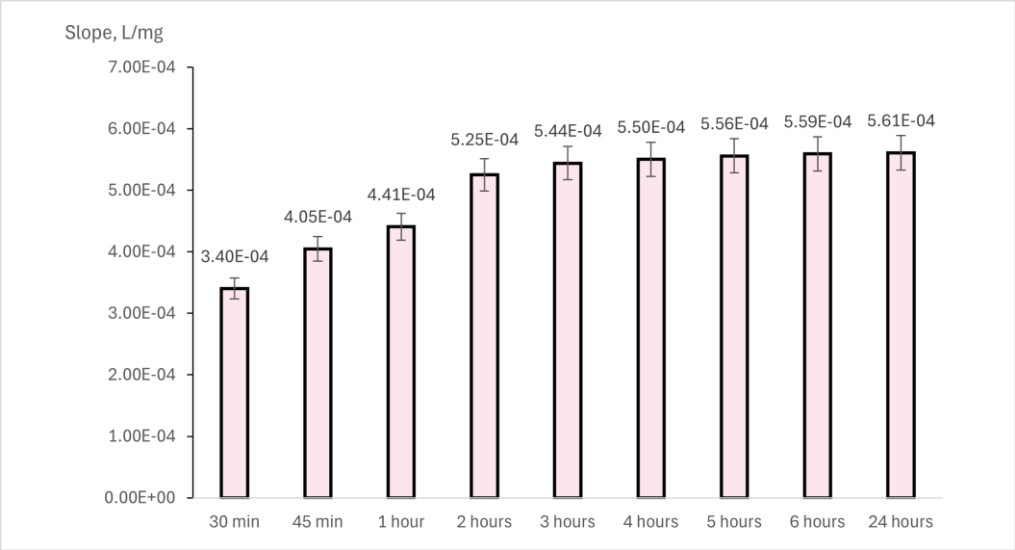

Figure 17: Stability of the coloured product over time.

3.5. Analytical Features

The analytical features of the developed µPAD for glucose determination are summarized in Table 3. A dynamic range of 22.0–220 mg/L was established, covering both physiological and pathological glucose concentrations in dogs. From six calibration curves, the limit of detection (LOD) was estimated at 6.70 mg/L and the limit of quantification (LOQ) at 22.3 mg/L, which defines the sensitivity of the method. Precision was evaluated through calibration curves obtained on four different days, with an interday relative standard deviation (RSD) of 4%. The system required approximately 30 minutes for signal stabilization and measurement. Each µPAD consumed only 106 µg of o-dianisidine, 81.8 mg of ethanol, 1.08 mg of glucose oxidase (GOx, Type VII), 3.24 mg of

peroxidase (POX, Type I), 0.490 mg of sodium acetate, and 4.11 mg of potassium phosphate, demonstrating the low reagent demand and cost-effective nature of the device.

Table 3: Features of the developed µPAD for glucose determination; Limit of Detection (LOD); Limit of Quantification (LOQ); Relative Standard Deviation (RSD).

Dynamic Range	22,0-220 mg/L
Calibration curve* (A = slope ± SD × [Glucose] mg/L + intercept ± SD)	$A = 3.76 \times 10^{-4} \pm 2.50 \times 10^{-5}$ [Glucose] mg/L - $2.84 \times 10^{-4} \pm 8.40 \times 10^{-4}$
LOD*	6.70 mg/L
LOQ*	22.3 mg/L
Interday repeatability, slope RSD**	4%
Time to scan	30 minutes
Reagent consumption per µPad	0.106 mg o-dianisidine 81.8 mg ethanol 1.08 mg GOx (Type VII) 3.24 mg POX (Type I) 0.490 mg sodium acetate 4.11 mg potassium phosphate

*n=6 calibration curves; **n= 4 calibration curves

3.6. Application of the developed µPAD

In this study, four canine saliva samples were analyzed with the µPAD system. The initial saliva samples did not produce a detectable response, as no colour change was observed. To overcome this limitation, controlled additions of glucose were carried out as described in Table 2, and the corresponding colourimetric responses obtained on the µPAD are shown in Figure 18 (ii). After the first addition (samples A1 and B1), the theoretical baseline concentration of glucose was estimated at 18.3 mg/L, which represents the minimum concentration expected in these samples. The µPAD

measurements confirmed this estimation, yielding 18.5 mg/L for A1 and 19.2 mg/L for B1, corresponding to recoveries of 101% and 105%, respectively. Following the second addition (samples A2 and B2), the expected glucose concentration was 68.8 mg/L. The µPAD interpolated values were 70.1 mg/L for A2 and 80.6 mg/L for B2, with recoveries of 102% and 117%. Recovery values close to 100% indicate that the method provides accurate quantification, while values above 100% reflect a tendency of the system to slightly overestimate the actual concentration, especially at higher spiking levels (Table 4).

The glucose concentrations estimated for samples A and B also suggest that the dogs from which the saliva was collected were likely not diabetic. As mentioned before, it is known that salivary glucose levels typically range around 2.5 mg/dL in non-diabetic dogs and up to 25.5 mg/dL in diabetic ones [8]. The concentrations interpolated with the µPAD fall within or only slightly above the expected physiological range for healthy dogs and remain well below the values usually associated with diabetes. These findings therefore reinforce the assumption that the animals sampled were clinically healthy.

Complementary analyses were also performed with the Megazyme D-Glucose HK Assay Kit [37] using the last two samples. However, no detectable signal was obtained, despite the kit's reported detection limit of approximately 0.66 mg/L, which is lower than in the µPAD (6.70 mg/L). This apparent contradiction is likely due to practical limitations like the very small saliva volumes available and the complex composition of canine saliva. These factors may have inhibited or interfered with the enzymatic reactions of the kit, preventing glucose detection even if small amounts were present.

Taken together, these results demonstrate that the µPAD system was capable of detecting glucose in spiked canine saliva with satisfactory accuracy, while also highlighting the methodological limitations of the present study. Access to larger sample volumes, clinical information on the animals, and a broader range of subjects would be required to confirm the robustness and diagnostic applicability of this approach.

Table 4: Expected and measured glucose concentrations in canine saliva samples analyzed with the µPAD, with corresponding recovery values.

Sample	Condition	Expected [Glucose] (mg/L)	µPAD [Glucose] (mg/L)	Recovery (%)
A1	1st addition	18.3	18.5	101
A2	2nd addition	68.8	70.1	102
B1	1st addition	18.3	19.2	105
B2	2nd addition	68.8	80.6	117

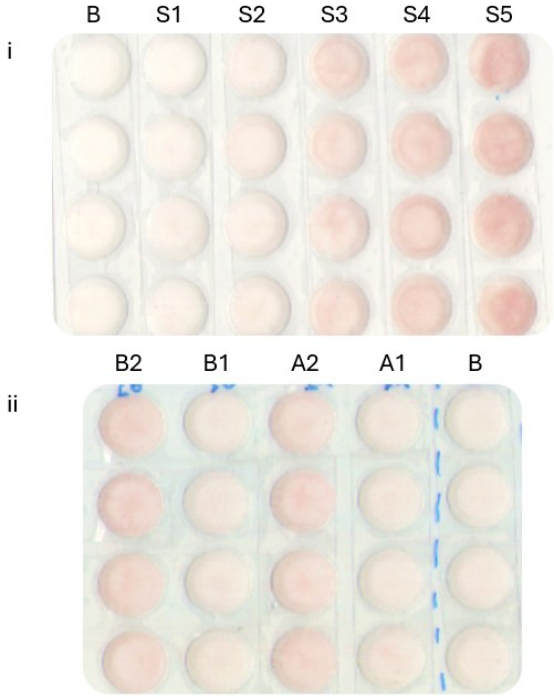

Figure 18: Colorimetric response on the µPAD. (i) Blank (B) and glucose standards S1–S5 (increasing concentrations). (ii) Canine saliva samples (A1, A2, B1, B2) and blank (B).

3.7. Cost Analysis

The cost analysis showed that the fabrication of a single µPAD costs approximately €4.66 (Table 5). The materials required for the device construction, including the filter paper and the lamination pouch, represented only a minor fraction of the total cost (€0.29 and €0.04, respectively). Similarly, the contribution of the chemical reagents, calculated on a mass basis, was negligible (<€0.01 per device). In contrast, the enzymes (glucose oxidase and peroxidase) were by far the dominant cost factor, accounting for over 90% of the total expense (€4.32 per µPAD). This is primarily due to their high commercial prices, since they are marketed based on enzymatic activity units rather than weight.

Despite this, the overall production cost remains affordable for laboratory-scale fabrication and could be further reduced in large-scale manufacturing. Buying enzymes in larger quantities, using recombinant or partially purified forms, or optimizing assay conditions to minimize enzyme consumption could significantly lower costs. Therefore, despite the strong influence of enzyme prices, the developed µPAD can still be considered a low-cost and promising platform for glucose detection in point-of-care diagnostics.

Table 5: Summary of the estimated costs for the fabrication of one µPAD, including paper substrates, lamination, chemical reagents, and enzymes. Detailed calculations are provided in Appendix B.

Category	Cost (€)
Paper (total)	0.29
Lamination pouch (1 unit)	0.04
Reagents (mass-based)	0.0048
Enzymes (GOx + Pox)	4.32
Total per µPAD	4.66

4. Conclusion and Future Work

In this work, a paper-based microfluidic device (μPAD) for the quantitative determination of glucose in canine saliva was successfully developed and optimized as a non-invasive alternative to conventional blood-based monitoring methods. The enzymatic system, based on glucose oxidase, peroxidase, and o-dianisidine, demonstrated good sensitivity and reproducibility, with detection limits compatible with the physiological and pathological glucose ranges reported for dogs. The introduction of a protective paper layer effectively overcame initial challenges related to enzyme stability during lamination, resulting in a robust, low-cost, and user-friendly design. Tests with real saliva samples confirmed the applicability of the μPAD. However, they were limited by the reduced number and volume of samples available and the absence of clinical information regarding the animals. Despite these limitations, the results validate the feasibility of this platform as a promising diagnostic tool that is cost-effective and focused on animal welfare. Future studies should cover larger sample sets, clinical validation across diverse animal populations, and digital integration for automated reading and continuous monitoring. Moreover, correlating salivary glucose concentrations with blood glucose levels from the same animals would be of particular interest, as it would provide valuable insights into the relationship between these two biological matrices and strengthen the validation of saliva as a reliable diagnostic fluid. In addition, urine could be investigated as another non-invasive matrix for comparative and complementary analysis. Overall, this work contributes to the advancement of paper-based biosensors in veterinary medicine and confirms that the developed μPAD fulfils the analytical requirements of a quantitative method. It demonstrates validated linearity, precision, and detection limits appropriate for saliva glucose determination within clinically relevant ranges, while emphasizing the importance of non-invasive and accessible solutions for managing chronic diseases in companion animals.

5. References

[1] P. J. Hantzidiamantis, A. O. Awosika, and S. L. Lappin, *Physiology, Glucose*. 2025.

[2] "The Prevalence of Diabetes in Pets." Accessed: Sep. 20, 2025. [Online]. Available: https://oakforestvet.com/the-prevalence-of-diabetes-in-pets/

[3] E. Behrend, A. Holford, P. Lathan, R. Rucinsky, and R. Schulman, "2018 AAHA Diabetes Management Guidelines for Dogs and Cats," *J Am Anim Hosp Assoc*, vol. 54, no. 1, pp. 1–21, Jan. 2018, doi: 10.5326/JAAHA-MS-6822.

[4] T. Whitbread, "Urinalysis — Diagnostic Procedures for the Private Practice Laboratory," *Merck Veterinary Manual*, Jun. 2025. [Online]. Available: https://www.merckvetmanual.com/clinical-pathology-and-procedures/diagnostic-procedures-for-the-private-practice-laboratory/urinalysis. [Accessed: Oct. 16, 2025].

[5] M. Hoenig, "Comparative aspects of diabetes mellitus in dogs and cats," *Mol Cell Endocrinol*, vol. 197, no. 1–2, pp. 221–229, Nov. 2002, doi: 10.1016/S0303-7207(02)00264-2.

[6] "Diabetes in Dogs and Cats." Accessed: Sep. 20, 2025. [Online]. Available: https://www.plantationpethealthcenter.com/veterinary-internal-medicine/diabetes-dogs-cats/

[7] P. Rzymski and B. Poniedzialek, "Blood glucose level as an insufficient indicator of feline diabetes mellitus: a case report," *Vet Med (Praha)*, vol. 58, no. 7, pp. 385–387, Jul. 2013, doi: 10.17221/6920-VETMED.

[8] A. Muñoz-Prieto, D. Escribano, J. J. Cerón, S. Martínez-Subiela, and A. Tvarijonaviciute, "Glucose, fructosamine, and insulin measurements in saliva of dogs: variations after an experimental glucose administration," *Domest Anim Endocrinol*, vol. 66, pp. 64–71, Jan. 2019, doi: 10.1016/j.domaniend.2018.10.002.

[9] B. Beerda, M. B. H. Schilder, N. S. C. R. M. Janssen, and J. A. Mol, "The Use of Saliva Cortisol, Urinary Cortisol, and Catecholamine Measurements for a Noninvasive Assessment of Stress Responses in Dogs," *Horm Behav*, vol. 30, no. 3, pp. 272–279, Sep. 1996, doi: 10.1006/hbeh.1996.0033.

[10] J. Wojtaś, M. Karpiński, and P. Czyżowski, “Salivary Cortisol Interactions in Search and Rescue Dogs and Their Handlers,” *Animals*, vol. 10, no. 4, p. 595, Apr. 2020, doi: 10.3390/ani10040595.

[11] A. Surdu *et al.*, “Saliva as a Diagnostic Tool for Systemic Diseases—A Narrative Review,” *Medicina (B Aires)*, vol. 61, no. 2, p. 243, Jan. 2025, doi: 10.3390/medicina61020243.

[12] C. M. M. Lensen, C. P. H. Moons, and C. Diederich, “Saliva sampling in dogs: How to select the most appropriate procedure for your study,” *Journal of Veterinary Behavior*, vol. 10, no. 6, pp. 504–512, Nov. 2015, doi: 10.1016/j.jveb.2015.08.006.

[13] Z. Yao *et al.*, “Paper-based sensors for diagnostics, human activity monitoring, food safety and environmental detection,” *Sensors & Diagnostics*, vol. 1, no. 3, pp. 312–342, 2022, doi: 10.1039/D2SD00017B.

[14] G. G. Morbioli, T. Mazzu-Nascimento, A. M. Stockton, and E. Carrilho, “Technical aspects and challenges of colorimetric detection with microfluidic paper-based analytical devices (μPADs) - A review,” *Anal Chim Acta*, vol. 970, pp. 1–22, Jun. 2017, doi: 10.1016/j.aca.2017.03.037.

[15] A. W. Martinez, S. T. Phillips, G. M. Whitesides, and E. Carrilho, “Diagnostics for the developing world: Microfluidic paper-based analytical devices,” *Anal Chem*, vol. 82, no. 1, pp. 3–10, 2010, doi: 10.1021/ac9013989.

[16] D. M. Cate, J. A. Adkins, J. Mettakoonpitak, and C. S. Henry, “Recent Developments in Paper-Based Microfluidic Devices,” *Anal Chem*, vol. 87, no. 1, pp. 19–41, Jan. 2015, doi: 10.1021/ac503968p.

[17] S. Liu, W. Su, and X. Ding, “A Review on Microfluidic Paper-Based Analytical Devices for Glucose Detection,” *Sensors*, vol. 16, no. 12, p. 2086, Dec. 2016, doi: 10.3390/s16122086.

[18] E. Gabriel, P. Garcia, F. Lopes, and W. Coltro, “Paper-Based Colorimetric Biosensor for Tear Glucose Measurements,” *Micromachines (Basel)*, vol. 8, no. 4, p. 104, Mar. 2017, doi: 10.3390/mi8040104.

[19] J. Xiao, Y. Liu, L. Su, D. Zhao, L. Zhao, and X. Zhang, “Microfluidic Chip-Based Wearable Colorimetric Sensor for Simple and Facile Detection of Sweat Glucose,” *Anal Chem*, vol. 91, no. 23, pp. 14803–14807, Dec. 2019, doi: 10.1021/acs.analchem.9b03110.

[20] A. K. Yetisen, M. S. Akram, and C. R. Lowe, “Paper-based microfluidic point-of-care diagnostic devices,” *Lab Chip*, vol. 13, no. 12, p. 2210, 2013, doi: 10.1039/c3lc50169h.

[21] O. Amor-Gutiérrez, E. Costa-Rama, and M. T. Fernández-Abedul, “Paper-Based Enzymatic Electrochemical Sensors for Glucose Determination,” *Sensors*, vol. 22, no. 16, p. 6232, Aug. 2022, doi: 10.3390/s22166232.

[22] F. T. S. M. Ferreira, A. O. S. S. Rangel, and R. B. R. Mesquita, “A Microfluidic Paper-Based Device for Monitoring Urease Activity in Saliva,” *Biosensors (Basel)*, vol. 15, no. 1, Jan. 2025, doi: 10.3390/bios15010048.

[23] F. T. S. M. Ferreira, R. B. R. Mesquita, and A. O. S. S. Rangel, “On-hand tool for ammonium and urea determination in saliva to monitor chronic kidney disease – Design of a couple of microfluidic paper-based devices,” *Microchemical Journal*, vol. 193, p. 109102, Oct. 2023, doi: 10.1016/j.microc.2023.109102.

[24] S. Altundemir, A. K. Uguz, and K. Ulgen, “A review on wax printed microfluidic paper-based devices for international health.,” *Biomicrofluidics*, vol. 11, no. 4, p. 041501, Jul. 2017, doi: 10.1063/1.4991504.

[25] X. Jiang and Z. H. Fan, “Fabrication and Operation of Paper-Based Analytical Devices,” *Annual Review of Analytical Chemistry*, vol. 9, no. 1, pp. 203–222, Jun. 2016, doi: 10.1146/annurev-anchem-071015-041714.

[26] R. A. G. de Oliveira, F. Camargo, N. C. Pesquero, and R. C. Faria, “A simple method to produce 2D and 3D microfluidic paper-based analytical devices for clinical analysis,” *Anal Chim Acta*, vol. 957, pp. 40–46, Mar. 2017, doi: 10.1016/j.aca.2017.01.002.

[27] A. B. Sözmen, A. E. Bayraktar, and A. Arslan-Yildiz, “Origami-inspired microfluidic paper-based analytical device (μPAD) for microorganism detection,” *Emergent Mater*, vol. 7, no. 6, pp. 2985–2993, Dec. 2024, doi: 10.1007/s42247-024-00775-1.

[28] S. Jaitpal and D. Paul, “Flow Control in Paper-Based Microfluidic Devices,” 2019, pp. 47–66. doi: 10.1007/978-981-15-0489-1_4.

[29] P. Aryal and C. S. Henry, “Advancements and challenges in microfluidic paper-based analytical devices: design, manufacturing, sustainability, and field applications,” *Frontiers in Lab on a Chip Technologies*, vol. 3, Dec. 2024, doi: 10.3389/frlct.2024.1467423.

[30] F. Ardakani and B. Hemmateenejad, “Challenges in the development of microfluidic paper–based analytical devices (μPADs),” Jul. 01, 2025, *Springer*. doi: 10.1007/s00604-025-07270-2.

[31] Anushka, A. Bandopadhyay, and P. K. Das, “Paper based microfluidic devices: a review of fabrication techniques and applications,” Jun. 01, 2023, *Springer Science and Business Media Deutschland GmbH*. doi: 10.1140/epjs/s11734-022-00727-y.

[32] B. Wang *et al.*, “Smartphone-based platforms implementing microfluidic detection with image-based artificial intelligence,” Dec. 01, 2023, *Nature Research*. doi: 10.1038/s41467-023-36017-x.

[33] G. Korir and M. Prakash, “Punch Card Programmable Microfluidics,” *PLoS One*, vol. 10, no. 3, p. e0115993, Mar. 2015, doi: 10.1371/journal.pone.0115993.

[34] F. T. S. M. ; R. A. O. S. S. ; M. R. B. R. Ferreira, “Design of paper-based analytical devices for chemical and biochemical assays of biomarkers in biological fluids of non-invasive collection,” in *XXVIII Encontro Galego-Português de Química: Livro de Resumos*, Santiago de Compostela: Colegio Oficial de Químicos de Galicia, 2024, p. 185.

[35] L. M. Hillscher, V. J. Liebich, O. Avrutina, M. Biesalski, and H. Kolmar, “Functional paper-based materials for diagnostics,” *ChemTexts*, vol. 7, no. 2, p. 14, Jun. 2021, doi: 10.1007/s40828-021-00139-w.

[36] G. R. Batista, C. R. G. Torres, B. Sener, T. Attin, and A. Wiegand, “Artificial Saliva Formulations versus Human Saliva Pretreatment in Dental Erosion Experiments,” *Caries Res*, vol. 50, no. 1, pp. 78–86, 2016, doi: 10.1159/000443188.

[37] Megazyme, “D-Glucose Assay Procedure (HK/G6P-DH Format).,” Bray, Ireland, 2020. Accessed: Sep. 20, 2025. [Online]. Available: https://www.megazyme.com

6. Appendix

A. Whatman Guideline for the cellulose filter papers

Typical Properties - Cellulose Filters

Grade	Particle Retention* Liquid (µm)	Air Flow Rate (s/100 mL/in²)	Ash (%)	Typical Thickness (µm)	Basis Weight (g/m²)	Wet Burst (psi)	Dry Burst (psi)	Tensile M/D Dry (N/15 mm)
Qualitative								
1	11	10.5	0.06	180	88	0.3	16	39.1
2	8	21	0.06	190	103	0.7	16	44.6
3	6	26	0.06	390	187	0.5	28	72
4	20-25	3.7	0.06	205	96	0.7	10	28.4
5	2.5	94	0.06	200	98	0.4	21	55.6
6	3	35	0.2	180	105	0.3	15	39.1

contd >

Grade	Particle Retention* Liquid (µm)	Air Flow Rate (s/100 mL/in²)	Ash (%)	Typical Thickness (µm)	Basis Weight (g/m²)	Wet Burst (psi)	Dry Burst (psi)	Tensile M/D Dry (N/15 mm)
General Purpose and Wet Strengthened Qualitative								
91	10	6.2	N/A	205	71	2	18	28
93	10	7	N/A	145	67	2.6	12	38
113	30	1.3	N/A	420	131	8	24	38.6
114	23	5.3	N/A	190	77	8.9	15	42.1
Ashless Quantitative								
40	8	19.3	0.007	210	92	0.5	16	46.7
41	20-25	3.4	0.007	215	84	0.3	10	27.2
42	2.5	107	0.007	200	100	0.7	25	55.8
43	16	8.9	0.007	220	96	0.6	12	38.2
44	3	57	0.007	176	77	0.4	44	39.4
Hardened Low Ash Quantitative								
50	2.7	96	0.015	115	97	9.1	33	84
52	7	11.4	0.015	175	101	8.3	24	71.5
54	20-25	4.2	0.015	185	92	9.4	18	57.6
Hardened Ashless Quantitative								
540	8	13.2	0.006	160	88	9	20	63
541	20-25	3.8	0.006	155	82	5.3	14	43.4
542	2.7	69	0.006	150	93	9.2	28	82.6

B. Cost analysis

Table 6: Paper cost calculations

Paper Grade	Disc Diameter (cm)	Discs per Sheet	Total Discs/Box	Box Price (€)	Price per Disc (€)	Discs per µPAD	Subtotal per µPAD (€)
Whatman 1	0.95	164	16400	20	0.00122	24	0.03
Whatman 42	0.95	164	16400	69	0.00421		0.10
Whatman 50	1.27	98	9800	65.6	0.00669		0.16

Table 7: Reagent cost calculations

Reagent	Used (mg)	Pack size (g)	Pack price (€)	Cost per µPAD (€)
o-Dianisidine	0.106	25	187	0.00079
Ethanol	81.8	1974	70.4	0.00292
Sodium acetate	0.49	1000	80	0.00004
Potassium phosphate	4.11	250	65.2	0.00107

*Ethanol mass calculated from the pack volumr (2.5L).

Table 8: Enzyme cost calculations

Enzyme	Used (mg)	Used per µPAD (mg)	Specific activity range (U/g)	Pack (U)	Pack (mg)	Pack price (€)	Cost per µPAD (€)
Glucose oxidase (Type VII)	3	1.08	248878	10000	40	73.9	2.00
Peroxidase (Type I)	9	3.24	0.08963	25000	278.9	200	2.32